1-1-2014

A distributed fiber vibration sensor utilizing dispersion induced walk-off effect in a unidirectional Mach-Zehnder interferometer

Qingming Chen

Chao Jin

Yuan Bao

Zhaohui Li

Jianping Li

See next page for additional authors

Authors

Qingming Chen, Chao Jin, Yuan Bao, Zhaohui Li, Jianping Li, Chao Lu, Liang Yang, and Guifang Li

A distributed fiber vibration sensor utilizing dispersion induced walk-off effect in a unidirectional Mach-Zehnder interferometer

Qingming Chen,[1] Chao Jin,[1,2] Yuan Bao,[1] Zhaohui Li,[1,*] Jianping Li,[1] Chao Lu,[2] Liang Yang,[3] and Guifang Li[4,5,6]

[1]*Institute of Photonics Technology, Jinan University, Guangzhou 510632, China*
[2] *Photonics Research Centre, The Hong Kong Polytechnic University, Hongkong, China*
[3] *Information Engineering College,Guangdong University of Technology,China*
[4] *CREOL, University of Central Florida, Orlando, FL 32816 USA*
[5] *Tianjin University, Tianjin, China*
[6]*li@creol.ucf.edu*
[*]*tlzh88@jnu.edu.cn*

Abstract: We propose and experimentally demonstrate a novel ultra-long range and sensitive distributed fiber vibration sensor. Only one unidirectional Mach-Zehnder interferometer (MZI) is employed in this scheme as the sensing element. In this sensor structure, we utilize chromatic dispersion-induced walk-off effect between the vibration signals sensed by two distributed feedback (DFB) lasers at different wavelengths to locate the vibration position. Vibration signals with frequencies up to 9MHz can be detected and the spatial resolution of 31m is achieved over 320km of the standard single mode fiber. Monitoring multiple vibration sources can also be realized using this scheme.

OCIS codes: (060.2370) Fiber optics sensors; (120.0280) Remote sensing and sensors.

References and links

1. X. Fang, "A variable-loop Sagnac interferometer for distributed impact sensing," J. Lightwave Technol. **14**(10), 2250–2254 (1996).
2. T. Lan, C. Zhang, L. Li, G. Luo, and C. Li, "Perimeter security system based on fiber optic disturbance sensor," Proc. SPIE 6830, Advanced Sensor Systems and Applications **III**, 68300J (2007).
3. J. P. Dakin, D. A. J. Pearce, A. P. Strong, and C. A. Wade, "A novel distributed optical fibre sensing system enabling location of disturbances in a Sagnac loop interferometer," Proc. SPIE **838**, 325–328 (1987).
4. A. A. Chtcherbakov, P. L. Swart, S. J. Spammer, and B. M. Lacquet, "Modified Sagnac/Mach-Zehnder interferometer for distributed disturbance sensing," Microw. Opt. Technol. Lett. **20**(1), 34–36 (1999).
5. S. J. Russell, K. R. C. Brady, and J. P. Dakin, "Real-time location of multiple time-varying strain disturbances acting over a 40km fiber section using a novel dual-Sagnac interferometer," J. Lightwave Technol. **19**(2), 205–213 (2001).
6. X. Fang, "Fiber-optic distributed sensing by a two-loop Sagnac interferometer," Opt. Lett. **21**(6), 444–446 (1996).
7. M. Kondrat, M. Szustakowski, N. Palka, W. Ciurapinski, and M. Zyczkowski, "A Sagnac-Michelson fiber optic interferometer: signal processing for disturtance localization," Opto-Electron. Rev. **15**(3), 127–132 (2007).
8. X. Hong, J. Wu, C. Zuo, F. Liu, H. Guo, and K. Xu, "Dual Michelson interferometers for distributed vibration detection," Appl. Opt. **50**(22), 4333–4338 (2011).
9. B. Kizlik, "Fibre optic distributed sensor in Mach-Zehnder interferometer configuration," in Modern Problems of Radio Engineering, TCSET, Proceedings of the International Conference (2002), 128–130.
10. L. Yuan and Y. Dong, "Loop topology based white light interferometric fiber optic sensor network for application of perimeter security," Photonic Sensors **1**(3), 260–267 (2011).
11. J. C. Juarez, E. W. Maier, K. N. Choi, and H. F. Taylor, "Distributed fiber-optic intrusion sensor system," J. Lightwave Technol. **23**(6), 2081–2087 (2005).
12. Y. Lu, T. Zhu, L. Chen, and X. Bao, "Distributed vibration sensor based on coherent detection of phase-OTDR," J. Lightwave Technol. **28**, 3243–3249 (2010).
13. R. Bernini, A. Minardo, and L. Zeni, "Dynamic strain measurement in optical fibers by stimulated Brillouin scattering," Opt. Lett. **34**(17), 2613–2615 (2009).

14. Z. Zhang and X. Bao, "Distributed optical fiber vibration sensor based on spectrum analysis of Polarization-OTDR system," Opt. Express **16**(14), 10240–10247 (2008).
15. T. Zhu, Q. He, X. Xiao, and X. Bao, "Modulated pulses based distributed vibration sensing with high frequency response and spatial resolution," Opt. Express **21**(3), 2953–2963 (2013).
16. S. M. Kay, *Fundamentals of Statistical Signal Processing: Estimation Theory* (Prentice-Hall, 1993).

1. Introduction

Distributed fiber sensing systems have been investigated and deployed to detect and locate external environmental disturbances along the fiber link for some time. They can be used to interrogate slowly-varying quantities, such as temperature or strain. Distributed optical fiber sensor systems can also be used to measure the dynamic processes, such as a walking person, vibration of engines, crack of block buildings, border intrusion or pipeline leakage. For distributed optical fiber sensing systems demonstrated so far, a large number of signals are acquired and processed in order to obtain a reasonable signal to noise ratio (SNR), so the acquisition time is typically on the order of few minutes. They fall into two categories, one is based on optical fiber interferometers [1–10] and the other is based on optical backscattering [11–15].

A variety of fiber interferometer-based configurations have been proposed to realize distributed vibration signal measurement, such as the optical Sagnac loop [1], the Mach-Zehnder interferometer (MZI) [2] and Michelson interferometer. In order to obtain the vibration location of distributed optical fiber sensor system, either modified optical interferometer structures are adopted or two kinds of optical interferometer structures are merged together, such as incorporating an MZI with a Sagnac loop [3], modified Sagnac/MZI [4], twin Sagnac interferometers [5,6], merged Sagnac-Michelson interferometers [7], dual Michelson interferometers [8], dual MZIs [9] and scanning MZI [10]. Due to the differences between correlated signals in separate interferometers caused by noises or changes of polarization states, both the spatial resolution and measurement range for twin optical interferometer structures are limited. A 40m spatial resolution over 6km sensing fiber has been achieved using a Sagnac-Michelson interferometer [7], and a 102m spatial resolution over 4012m fiber has been achieved using a dual Michelson interferometer structure [8]. These systems cannot be used for long distance, high spatial resolution and high vibration frequency applications. In addition, monitoring of multiple vibration sources cannot be realized with these interferometer based schemes.

Optical backscattering effects, such as Rayleigh and Brillouin backscattering, have also been utilized to realize the distributed vibration sensing systems [11–13], e.g. the phase-sensitive optical time domain reflectometer (φ-OTDR) system. Another kind of distributed vibration sensing system is based on polarization OTDR (P-OTDR), which has achieved 10m spatial resolution in 1km sensing range [14]. The spatial resolution of these kinds of sensing systems is determined by the pulse width of the injected light. The distributed vibration sensing system based on optical backscattering or polarization effects need to acquire a great number of waveforms to obtain a high SNR through averaging.

Recently, a distributed vibration sensing system combining the advantages of optical interferometer and φ-OTDR system realizes a high frequency response and accurate location simultaneously [15]. However, this system is quite complex.

In this paper, we propose and experimentally demonstrate a novel ultra-long range and sensitive distributed fiber vibration sensor. Only one single MZI structure and two continuous-wave (CW) distributed feedback (DFB) lasers are employed in this scheme. In this sensor structure, we utilize the chromatic dispersion-induced walk-off of vibration signal sensed by the two DFB lasers with different wavelengths to locate the vibration position. The vibration signal with frequency of up to 9MHz can be been measured and the spatial resolution of 31m is achieved over 320km standard single mode fiber (SSMF), which has the longest measurement range for the reported distributed vibration sensing system to our knowledge. Monitoring of multiple vibration sources can also be realized in this scheme. In addition, frequency response characterization of distributed vibration sensing system is also analyzed using digital signal processing method.

2. Operation principle, experimental setup and signal processing

2.1 Operation principle and experimental setup

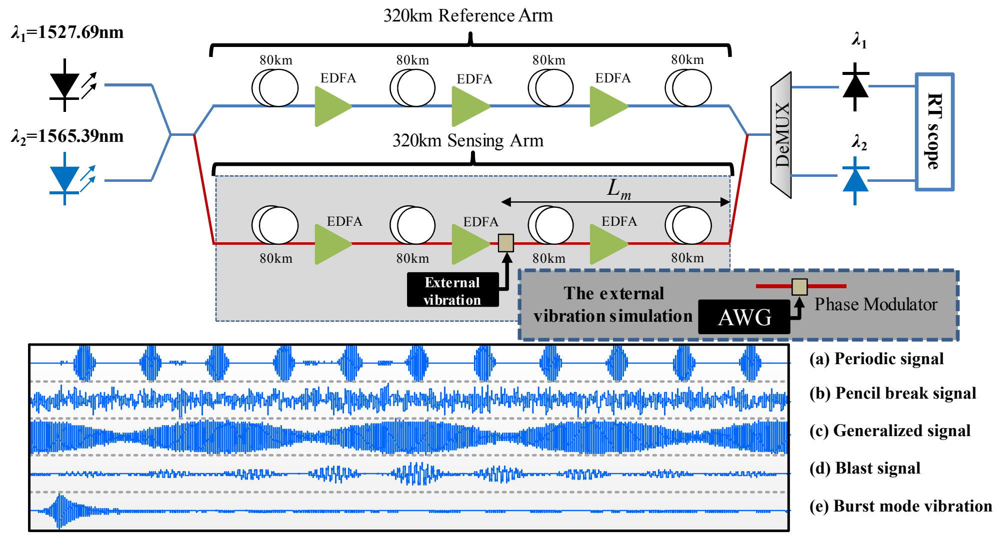

Fig. 1. Operation principle and experimental setup of distributed vibration sensor.

The operation principle of the proposed distributed fiber vibration sensor is shown in Fig. 1, in which only a single MZI and two CW DFB lasers are employed. The configuration of MZI consists of two arms, one is a sensing arm and another is a reference arm. Both arms have nearly the same length of 320km SSMF. We use Erbium doped fiber amplifiers (EDFAs) to compensate the link loss every 80km of SSMF in both arms in order to extend the sensor range. Two CW DFB lasers with the center wavelength at 1527.69nm and 1565.39nm respectively are launched into the MZI through an optical coupler and then separated from each other through a wavelength division multiplexed (WDM) DeMUX at the output of the MZI. The output signals carrying vibration information are mixed with the reference lasers, detected by two photo-detectors (PDs) and input into a real-time oscilloscope for signal acquisition and processing. Different types of external vibration signals from an arbitrary waveform generator (AWG) are imposed onto one of the arm of MZI through a phase modulator (PM). Here, we use a PM to replace the PZT to impose a phase signal in order to study the high frequency response of the distributed fiber vibration sensing system. We have constructed five types of vibrations signal to simulate different practical cases: (a) a periodic signal to simulate periodical process, (b) a pencil-break signal with frequency up to 3MHz to simulate cracks in buildings, (c) a generalized signal, (d) blast signal and (e) burst vibration.

As the vibration information is imposed onto the sensing arm, DFB laser signals at different wavelength in the sensing arm will experience the same phase change. While the DFB lasers in the reference arm will not be influenced by any external vibration signal disturbance. However, due to the chromatic dispersion induced walk-off effect in the SSMF, the vibration signal carried on DFB lasers with different wavelength will reach the end of the fiber link at different time. As a result, we can obtain the location of vibration through analyzing the relative time delay between the vibration signals detected by two PDs.

#193992 - $15.00 USD Received 16 Jul 2013; revised 6 Jan 2014; accepted 14 Jan 2014; published 27 Jan 2014

As shown in Fig. 1, we assume that the vibration signal can be imposed at an arbitrary point (L_m to the end of fiber link) in the sensing arm of MZI. Although the laser signals with different wavelengths are parallel transmitted in the same MZI, they are individually detected. Considering for the single wavelength for simplicity, the optical signal coming out from the reference arm can be described as $E_r = A_r\exp(j\omega t)$, where A_r is the complex amplitude and ω is the angular frequency. Similarly the output signal coming out from the sensing arm can be described by $E_s = A_s\exp[j\omega t + \xi(t)]$, where A_s is the complex amplitude, and $\xi(t)$ is the phase change imposed by vibration signal. The output photo-currents can be written as follows,

$$I(t) = R\left[\mathrm{Re}\left(E_r + E_s\right)\right]^{MeanSquare} = R\left[\frac{1}{2}\left|A_r\right|^2 + \frac{1}{2}\left|A_s\right|^2 + \left|A_s A_r\right|\cos(\xi(t))\right] \tag{1}$$

where $[\bullet]^{MeanSquare}$ represents the mean square, $\mathrm{Re}(\bullet)$ is the real part and R represents the responsibility of the photo-diode. Since both optical signals at wavelength of λ_1 and λ_2 experience the same MZI and the same phase disturbance $\xi(t)$, the interference patterns detected by two PDs of each wavelength are nearly the same theoretically, as shown in Eq. (1), except the time delay induced by the chromatic dispersion in fiber. The walk-off effect between two output optical signals at different wavelength induced by chromatic dispersion can be expressed as $\Delta T = DL_m|\lambda_2 - \lambda_1|$, where D is the chromatic dispersion coefficient of SSMF. The position of the vibration signal can be easily determined by

$$L_m = \Delta T / D\,|\,\lambda_2 - \lambda_1\,|. \tag{2}$$

Therefore, in order to estimate the vibration position L_m, we can use a blind estimation program to estimate the time delay ΔT.

2.2 Signal processing in distributed vibration sensing system

We represent the two received signals sampled by the real-time oscilloscope as $x_1(t) = \alpha_1 I(t) + n_1(t)$ and $x_2(t) = \alpha_2 I(t - \Delta T) + n_2(t)$, where $n_1(t)$ and $n_2(t)$ are independent additive white Gaussian noises (AWGN), and ΔT is the chromatic dispersion induced walk-off effect of arriving time, α_1 and α_2 are the scaling factors related to the polarization mismatch, responsibility of the photo-diodes and the coupling coefficients of couplers.

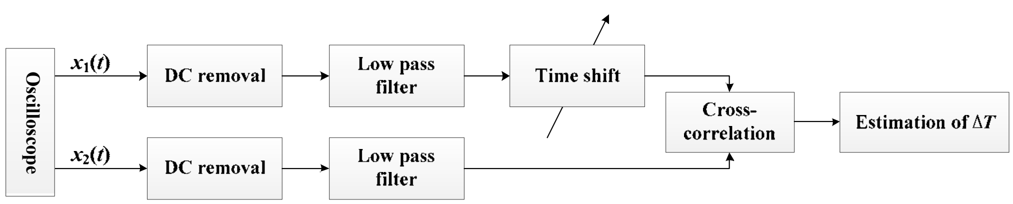

Fig. 2. Diagram of signal processing.

Therefore, we can use cross-correlator to estimate the target time delay ΔT. The signal processing diagram used in the distributed fiber vibration sensing system is shown in Fig. 2. First, the DC component of the detected vibration signals is removed. Then a digital low pass filter is used to filter out the out-of-band noise to improve the SNR and the performance of the correlator. The estimation of the walk-off time delay ΔT can be obtained by the peak position of the cross-correlation between $x_1(t)$ and $x_2(t)$. The location accuracy can be evaluated by the variance of ΔT and it depends on the SNR, which will degrade after propagation over such a long fiber link. The relationship between SNR and variance of ΔT is discussed in [16], and the Cramer-Rao lower bound (CRLB) is provided as follows,

#193992 - $15.00 USD Received 16 Jul 2013; revised 6 Jan 2014; accepted 14 Jan 2014; published 27 Jan 2014

$$Var(\Delta T) \geq \frac{1}{\frac{\varepsilon}{N_0/2} F^2} = \frac{1}{\text{SNR} \cdot F^2} \tag{3}$$

where N_0 is the power spectral density of the noise, ε is the vibration signal power, and F^2 is the mean square bandwidth of the vibration signal, which can be written as follows,

$$\varepsilon = \int I^2(t)dt \tag{4}$$

$$F^2 = \int (2\pi f)^2 \left|I(f)\right|^2 df \Big/ \int \left|I(f)\right|^2 df \tag{5}$$

where $I(f)$ is the Fourier transform of $I(t)$.

3. Simulation results

We first study the performance of the proposed distributed fiber vibration sensing system by simulation. The sensing and reference arm of the MZI are composed of three EDFAs and 320km SSMF. Each EDFA can provide a constant 16dB gain to the optical signal and the noise figure is 4dB. The chromatic dispersion coefficient of SSMF is set as 16ps/(nm·km). Two DFB lasers with center wavelength at 1527.69nm and 1565.39nm are used and the corresponding wavelength difference is 37.7nm. The simulation sample rate of the signal processing is set as 5GS/s and a spatial resolution about 331m is obtained. We select four test positions along the sensing arm of the MZI by imposing different kinds of vibration signals through a PM.

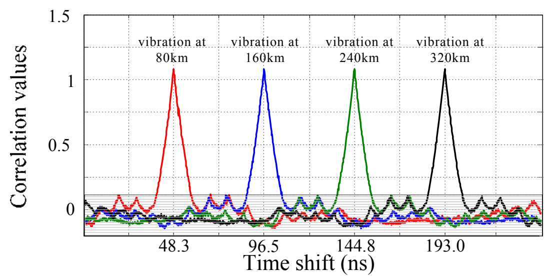

Fig. 3. Cross-correlation values of burst mode vibration signal for different locations.

Figure 3 shows the different cross-correlation values as the burst mode vibration signal is placed at different location of sensing arm of the MZI. The tested burst mode vibration signal is composed of 1MHz sinusoidal signal and lasts for 15μs. It can be seen that the correlation peak can be identified clearly and the walk-off delay moves according to the vibration location.

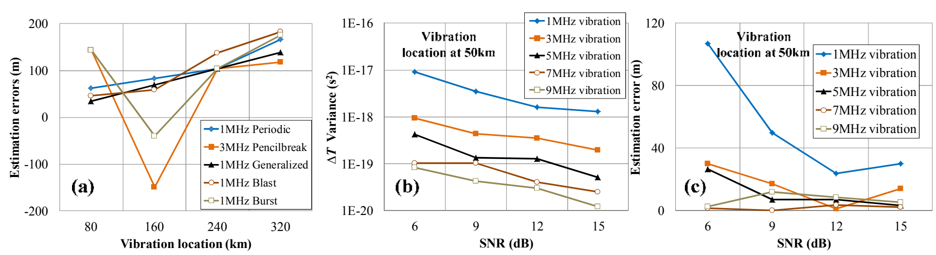

Fig. 4. (a) The location error results for variable vibration signals (b) and (c) estimation variance of time delay and location errors at different SNRs and vibration frequency as the vibration source placed at 50km, respectively.

#193992 - $15.00 USD Received 16 Jul 2013; revised 6 Jan 2014; accepted 14 Jan 2014; published 27 Jan 2014

The performance of the MZI-based vibration sensor for various vibration signals are evaluated and Fig. 4(a) shows that the measurement error is less than 190m along the 320km fiber link. The estimated variances of time delay and location errors versus the SNR and vibration frequency are plotted in Figs. 4(b) and 4(c), respectively. It can be seen that higher SNR and higher frequency of the vibration will reduce the estimation variance and improve accuracy by using the cross-correlator to estimate the walk-off time delay ΔT. The performance of low frequency vibration sensing is influenced by the phase noise of the laser and it can be improved by employing lasers with narrower line-width.

4. Experimental results

4.1 Single vibration source location

A proof-of-concept experiment has also been demonstrated to verify the proposed long-distance fiber vibration sensing method. Here, the generalized signal is used as the vibration signal and the optical fiber has a dispersion coefficient about 17ps/(nm·km). To improve the spatial resolution, the sampling rate of the scope is set 50GS/s, yielding a spatial resolution about 31m.

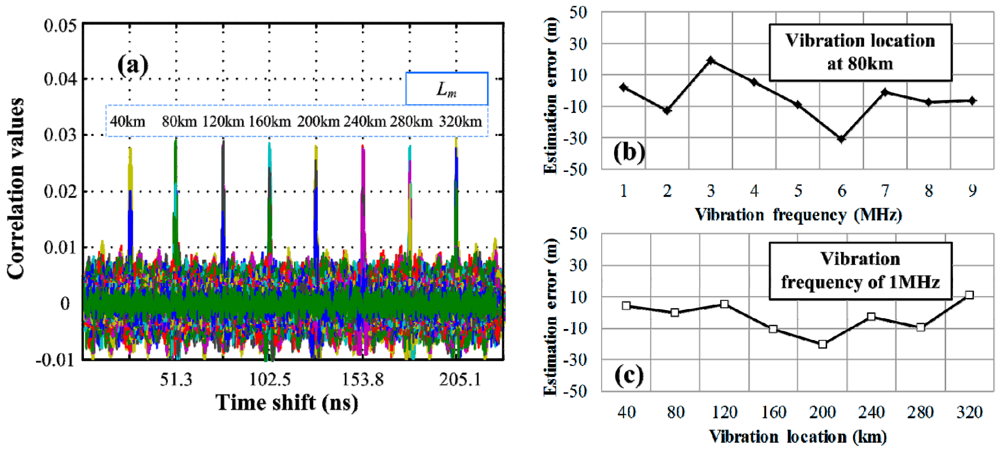

Fig. 5. (a) Cross-correlation values output from the correlator. The estimation errors obtained from the experiment at different (b) vibration frequencies and (c) vibration locations.

Figure 5(a) shows the superimposed cross-correlation values when the vibration source is placed at variable locations. It can be seen that the correlation peak is sharper since the spatial resolution is higher than the simulation and 3MHz vibration source is employed. Besides, the location error versus variable vibration frequency and arbitrary vibration locations are also tested and shown in Figs. 5(b) and 5(c), respectively. In order to improve the estimation performance, the experimental results are obtained by average of 100 acquisitions. From these results, it can be found that the MZI-based vibration sensor can reach up a high vibration frequency response to 9MHz and the long distance of 320km distribution fiber sensing is achieved successfully with a superior accuracy of ± 50m through averaging.

4.2 Dual vibration source location

To evaluate the monitoring performance of multiple vibration sources, two vibration sources are placed on the sensing arm of MZI, one at 80km and another at 240km. Two correlation peaks corresponding to the two vibration locations are clearly observed in the superimposed cross-correlation plotted in Fig. 6. Less than 50m location error is obtained after average of 100 correlation traces.

#193992 - $15.00 USD Received 16 Jul 2013; revised 6 Jan 2014; accepted 14 Jan 2014; published 27 Jan 2014

However, if the two vibration events occur too closely, the location performance will be influenced, so that there is a measurable blind zone in this MZI sensor. Since the width of the correlation peaks in Fig. 6 is 1.5ns, the blind zone should be 2340m. However, we still can use longer data samples for correlation calculation and it can improve the roll-off of the correlation peaks.

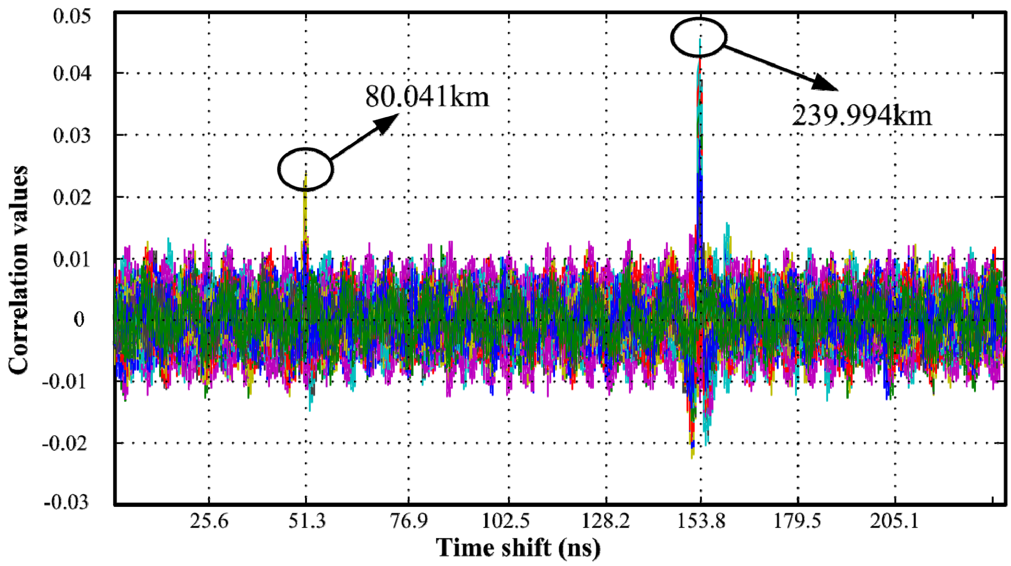

Fig. 6. Superimposed cross-correlation values for dual vibration signals.

4.3 Temperature variation and other environmental influence

Since the environmental changes will influence the vibration sensing performance of the proposed MZI-based sensor, it should be carefully deployed, e.g. keep the sensing arm in a stable place and avoid the fiber exposure to the air directly. Besides, considering the fiber dispersion changes slowly with the temperature variation, we can calibrate the dispersion coefficient by placing several fixed vibration sources uniformly along the sensing arm and activating the vibration spots and MZI sensor every one or two hours.

5. Conclusion

In this paper, a distributed fiber vibration sensing system has been theoretically studied and experimentally demonstrated utilizing a single Mach-Zehnder interferometer. The proposed sensor configuration is promising for ultra-long range and high frequency response distributed fiber vibration sensing. A 31m spatial resolution is achieved over a 320km sensing range. The vibration signals with frequency of up to 9MHz can be detected. Multiple vibration sources monitoring has also been demonstrated using this scheme.

Acknowledgments

The authors would like to acknowledge the support of National Basic Research Programme of China (973) project (No.2012CB315603), National Natural Science Foundation of China (NSFC) under Grant No.61001101, and New Century Excellent Talents in University (NCET-12-0679).